



Research article

Quantitative generation of microfluidic flow by using optically driven microspheres

Songyu Hu¹, Ruifeng Hu², Liping Tang¹, Weiwei Jiang³ and Banglin Deng^{1*}

¹ College of Mechatronics and Control Engineering, Shenzhen University, Shenzhen 518060, China

² Department of Mechanical Engineering and Materials Science, University of Pittsburgh, Pittsburgh, PA 15260, USA

³ College of Computer Science & Technology, Zhejiang University of Technology, Hangzhou 310023, China

* **Correspondence:** Email: dengbanglin123@126.com; Tel: +8675526531066; Fax: +8675526536224.

Abstract: Microfluidic flow generation plays a fundamental role in microfluidic systems and shows potential for applications in basic biology and clinical medicine. In this study, an enabling technology is proposed to quantitatively generate microfluid flow through the automatic movement of a microsphere in liquid by using optical tweezers. A closed-loop control strategy with visual servoing feedback is introduced to achieve high precision and robustness. The theoretical solution of the generated microfluid is obtained on the basis of Stokes equations. An experimental method is proposed, and experiments are performed to verify the effectiveness of our approach. This method does not impose any dedicated fabrication of microtool, and the microfluidic flow can be dexterously adjusted by controlling the direction, speed, and distance of the microsphere from a target location. To the best of our knowledge, this is the first demonstration of optically actuating liquids through the translational movement of microspheres with closed-loop control. The proposed method will be useful in various biomedical applications needing quantitative, precise and controllable localized microfluid.

Keywords: microfluidic flow; microfluidic system; theoretical solution; optical tweezers; optical trap; microsphere

Nomenclature: a : Radius of the microsphere; \mathbf{q} : Position of the microsphere; \mathbf{c} : Controller; \mathbf{q}^d : Desired position of the microsphere; \mathbf{e} : Position error of the microsphere; r : Distance from sphere center to target location; F_{drag} : Drag force; r_0 : Critical value; $F_{trapping}$: Trapping force; U : Velocity magnitude of the microsphere; k : Stiffness of the optical trap; \mathbf{V} : Fluid flow velocity; K_i : Integrating gain; x : Offset of the cell from the trap; K_p : Proportional gain; β : Drag coefficient of the liquid; \mathbf{l} : Position of the optical trap; ζ : Time variable.

1. Introduction

Microfluidic systems are miniaturized factories that can manipulate fluids in micro- and nano-metric scales [1]. In comparison with conventional macroscopic systems, microfluidic systems have attracted increasing attention for their advantages, including enhancing processing accuracy, reducing material consumption, and saving cost. In biomedical engineering, the ability to handle small volumes of biological samples and reagents enables many innovative assays, especially when a sample is precious and rare. Microfluidic systems have shown great potential for applications in rapid diagnosis [2,3], disease screening, drug delivery [4,5], cell biology [6,7], and synthetic biology [8,9].

Fluid flow actuation in micro- and nano-liter volumes is an essential step in microfluidic systems [10]. Considerable efforts have been devoted to generating precisely controllable fluid flow. One of the most popular methods used to control the movement of fluid flow is using a syringe pump to inject a small volume of liquid into a customized microfluidic chip fabricated by soft lithography techniques and poly-dimethylsiloxane [11–13]. This method is low cost and has been widely used to generate, mix, and cease fluid flow. However, it is mainly used to control liquid flow in the entire microfluid channel and has a relatively large time constant. Another type of actuation mechanism, involves the use of indirect micromanipulation techniques, such as electric fields [14], acoustic wave [15], magnetic fields [16–18], and optical fields [19], to control microfluidic flow. These physical fields drive microobjects to move in liquid and hence generate localized microfluidic flows surrounding these microobjects.

Among microtechniques, an optical field method, also named “optical tweezers” or “optical trap” [20], is a popular tool because of its high flexibility and precision. An optical trap can be used to trap and move microobjects ranging from tens of nanometers to tens of micrometers through radiation pressure from a focused laser beam (Figure 1). Optical force in the orders of a few piconewtons has been widely used to manipulate organelles, macromolecules, and cells in biology and medicine [21]. Optical traps have been used as an ideal small force gauge because the optical trapping force on a trapped microsphere as a particular laser power is linearly proportional to the deviation of the microsphere from the trap focus [22]. Many meaningful applications, including DNA stretching, cell deformability, and kinesin motion, have been explored.

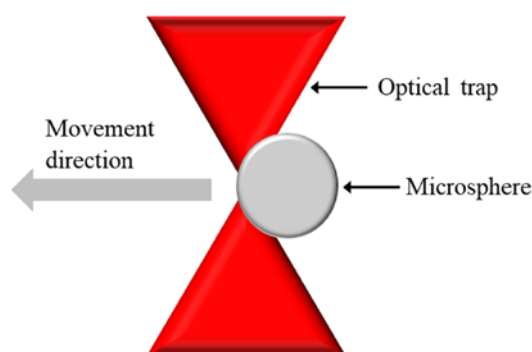


Figure 1. Schematic of moving a microsphere with an optical trap.

In microfluidic systems, optical traps have also been applied because of the perfect size matching between trapped microobjects and typical microfluidic chips and the force matching between the optical sensing force and the force involved in many microfluidic systems [23]. Marr et al. [24] created pumps and valves by using colloidal microspheres and via laser-initiated photopolymerization; they controlled the fluid flow within customized channels. Neale et al. [25] fabricated microgears, which can be rotated with an optical trap and function as micropumps to drive liquid, on the basis of the form birefringence principle. Maruo et al. [26] developed a lobed micropump by direct laser writing with a femtosecond laser beam. Two built-in rotors were cooperatively driven by the time-divided laser scanning and moved liquids. Recently, Būtaitė et al. [27] demonstrated a versatile hydrodynamic manipulation platform that utilizes multiple optically actuated microrotors. These innovative microtools have enabled the microfluidic control and exhibited good development and application perspective in micro-total-analysis systems. However, customized designs and fabrications, which are often expensive and time consuming, are necessary in the microtool-based methods. In addition, the usage of sophisticated microtools complicates the quantitative calculation and control of the generated fluid flows. Several microbeads-based methods have been reported as alternative techniques for addressing these issues. Leach et al. [28] rotated two birefringent vaterite particles with optical traps and generated flow to transport microbeads in a microfluidic channel. Wu et al. [29] generated localized microfluidic flow by rotating birefringent beads, which can control the direction of growth of individual nerve fibers. Both methods are based on the rotation of birefringent beads and only liquids at short distances can be driven. Furthermore, ensuring the precision and robustness of flow control is difficult because open-loop strategy is used in these demonstrations.

In this study, a new approach is proposed to quantitatively generate a localized microfluidic flow by automatically driving a microsphere to move in liquid. A closed-loop control strategy with visual servoing feedback is introduced to achieve high precision and robustness. This method does not require any special microfabrication facility, and the microfluidic flow can be quantitatively adjusted by controlling the direction, speed, and distance of the microsphere from target locations. To the best of our knowledge, this work is the first demonstration of optically driving liquids through translational movement of microspheres with closed-loop control. This work will contribute to the applications that need precise and adjustable tiny flows. Examples of such examples include exploring the behavior and function of single cell under fluid flows [29–32] and transporting materials in microfluidic systems.

The remainder of this paper is organized as follows. Section 2 presents the materials and

methods. Section 3 reports experimental results to demonstrate the proposed approach. Section 4 provides the summary and conclusions of this study.

2. Materials and methods

2.1. Automated movement of microsphere

2.1.1. Experimental setup

As described in our previous reports [33,34], a manipulation system of holographic optical tweezers (HOTs) is established on the basis of a motorized xyz stage and an inverted microscope (Ti-U, Nikon) with an objective (Plan Apo 60X/1.20 WI, Nikon) (Figure 2). A trapping beam is provided with a continuous laser beam with a maximum output of 3W at a wavelength of 1064 nm (V-I06C-3000 OEM J-series, Spectra Physics). The laser beam is first magnified by a telescope (Lens 1 and Lens 2) to match the beam width to the size of a spatial light modulator (SLM). Another telescope (Lens 3 and Lens 4) is then used to image the SLM plane onto the back focal plane of the microscope objective. In the process, the laser beam is split into multiple beams by the computer-generated hologram combined with the SLM, and each beam is focused into an individually controllable optical trap. A charge-coupled device (CCD) camera (Plan Apo 60X/1.20 WI, Nikon) is used to obtain the images of the workspace and enable the visual servo control by providing feedback of the microsphere. All the mechanical components are supported by an antivibration table in a clean room. The system software is developed using C++ language.

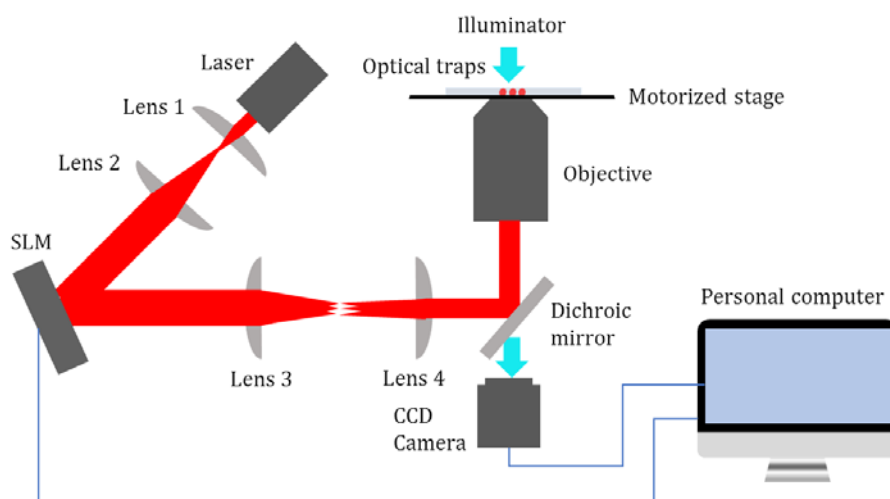


Figure 2. Schematic of the manipulation system of HOTs.

2.1.2. Generation of microfluidic flow

Figure 3 shows the schematic of generating microfluidic flow via the movement of a microsphere and provides a typical case of a cell next to a microsphere as an example. When a microsphere is moved in liquid by using optical tweezers, the microsphere “pulls” the surrounding

liquid to flow with it, and the cell is subjected to microfluidic flow. The direction of the fluid flow can be adjusted by changing the direction of the movement of the microsphere, and the velocity of the flow can be regulated by controlling the movement speed and distance of the microsphere from the cell. A closed-loop control strategy with visual servoing feedback is introduced to automatically move the microsphere and to achieve high precision of the generated microfluidic flow.

2.1.3. Closed-loop control for optically moving a microsphere

Various control algorithms have been developed to transport microspheres with optical tweezers [35–38]. We introduce a feedforward plus PI-type controller in this study [33]. The dynamic equation of the trapped microsphere can be expressed as

$$0 = k(\mathbf{l} - \mathbf{q}) - \beta \dot{\mathbf{q}}, \|\mathbf{l} - \mathbf{q}\| \leq r_0, \quad (1)$$

where k is the stiffness of the optical trap, β is the drag coefficient of the liquid, and \mathbf{l} and \mathbf{q} are the position of the optical trap and the microspheres, respectively.

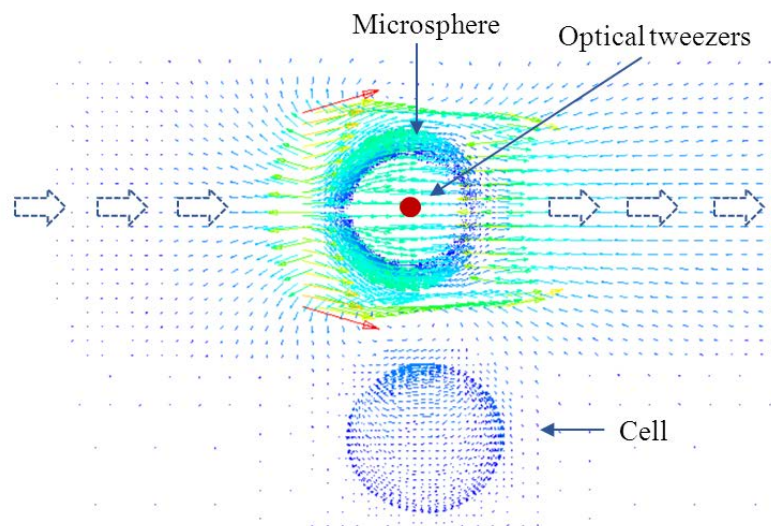


Figure 3. Generation of microfluidic flow by moving a microsphere with optical tweezers.

On the basis of the dynamic equation (1), we introduce a controller as follows:

$$\mathbf{l} - \mathbf{q} = \begin{cases} \mathbf{c}, & \|\mathbf{c}\| \leq r_0 \\ \frac{r_0}{\|\mathbf{c}\|} \mathbf{c}, & \|\mathbf{c}\| > r_0 \end{cases}, \quad (2)$$

where r_0 is a critical value introduced to prevent the escape of the microsphere from the optical trap in the movement; and \mathbf{c} is a feedforward plus PI-type controller described as follows:

$$\mathbf{c} = \frac{\beta}{k} \dot{\mathbf{q}}^d + \mathbf{q}^d + K_p \mathbf{e} + K_i \int_0^t \mathbf{e} d\zeta, \quad (3)$$

where K_p and K_i are positive feedback control gains, ζ is a time variable from 0 to t , and \mathbf{e} is the position error between the desired cell position \mathbf{q}^d and the actual cell position \mathbf{q} , expressed by

$$\mathbf{e} = \mathbf{q}^d - \mathbf{q}. \quad (4)$$

2.2. Theoretical solution of the generated microfluidic flow

A sphere of radius a is considered to be moving in a viscous incompressible liquid with a constant velocity magnitude U along the Z axis, and the influence of the vessel wall is disregarded. Adopting the spherical coordinates as shown in Figure 4 and according to the Stokes equations [39], we can obtain the generated fluid flow velocity \mathbf{V} as

$$\begin{cases} V_r = \frac{1}{2}U\left(\frac{3a}{r} - \frac{a^3}{r^3}\right)\cos\theta \\ V_\theta = -\frac{1}{4}U\left(\frac{a}{r} + \frac{a^3}{r^3}\right)\sin\theta \end{cases}, \quad (5)$$

where r is the distance from the sphere center to the target location.

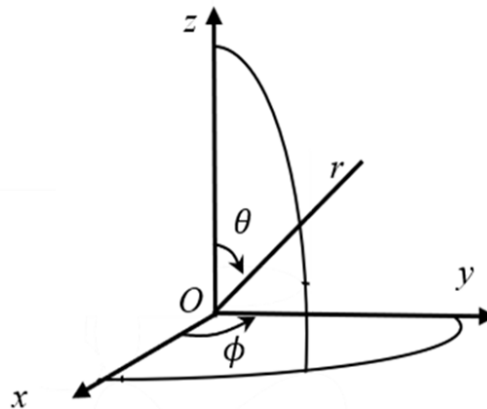


Figure 4. Schematic of spherical coordinates.

3. Experiments

3.1. Experimental principle

A drag force-based method is introduced to characterize the velocity of the generated

microfluidic flow. According to Stokes law, the drag force F_{drag} applied to a sphere by a fluid flow can be calculated as

$$F_{drag} = \beta \mathbf{V}, \quad (6)$$

where β is the drag coefficient and can be obtained experimentally. Therefore, if we obtain F_{drag} , we can determine the fluid flow velocity \mathbf{V} .

The schematic of characterizing F_{drag} is shown in Figure 5. A large microsphere and a small microsphere are trapped in liquid without other substances around them. For description simplicity, the small microsphere is called “cell” in this paper. The large microsphere is then moved in a straight line next to the cell, generating a microfluidic flow. Therefore, the cell is subjected to F_{drag} from the fluid flow and deviate from its original position. The cell stops in a new balanced position under F_{drag} and the trapping force from the optical trap, $F_{trapping}$. We can have

$$F_{drag} = F_{trapping} = k \cdot x, \quad (7)$$

where k is the stiffness of the optical trap, and x is the offset of the cell from the trap. We can obtain the stiffness k by conducting an experimental calibration [33] and determine the offset x by recording the positions of the cell through image processing. F_{drag} can be calculated according to equation (7).

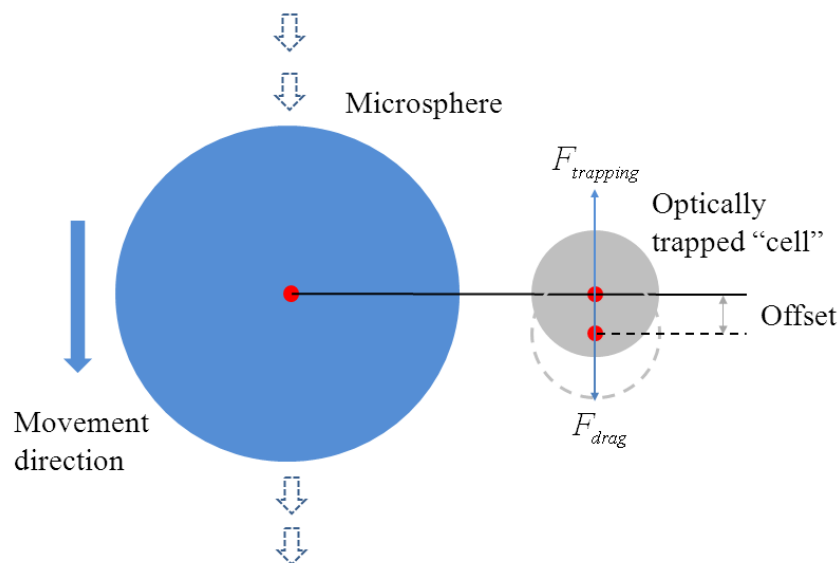


Figure 5. Schematic of characterizing the microfluidic flow.

3.2. Experimental results

Experiments were performed to compare the actual and theoretical microfluidic flow velocity. A microsphere with a radius of $12.0\ \mu\text{m}$ and a cell with a radius of $4.0\ \mu\text{m}$ were used, and the distance between the microsphere center and the cell center was $22.5\ \mu\text{m}$, indicating that the minimum distance between the surface of the microsphere and the cell was $18.5\ \mu\text{m}$ and that the maximum distance was $26.5\ \mu\text{m}$. The relative velocity between the microsphere and the cell was set to $40.0\ \mu\text{m/s}$. According to equation (5), we could calculate the velocity of the microfluids flowing through the cell, ranging from 25.1 to $33.5\ \mu\text{m/s}$.

The laser power on the cell was set to $0.2\ \text{W}$, and k/β obtained by calibration was $10.1\ \text{S}^{-1}$.

Figure 6 illustrates the process of the quantitative measurement of microfluidic flow velocity. As shown in Figures 6 (a) and (b), the microsphere moved in the negative direction along the y-axis. When the microsphere passed near the cell, the cell moved with the microsphere under F_{drag} from the generated fluid flow and $F_{trapping}$ from the optical trap. Figures 6 (c) and (d) show a similar measurement process of the microsphere moving in the positive direction along the y-axis. Figures 6 (b) and (d) illustrate that the cell was clearly moved and offsets were visible, implying that the microfluidic flow was successfully generated by the moved microsphere.

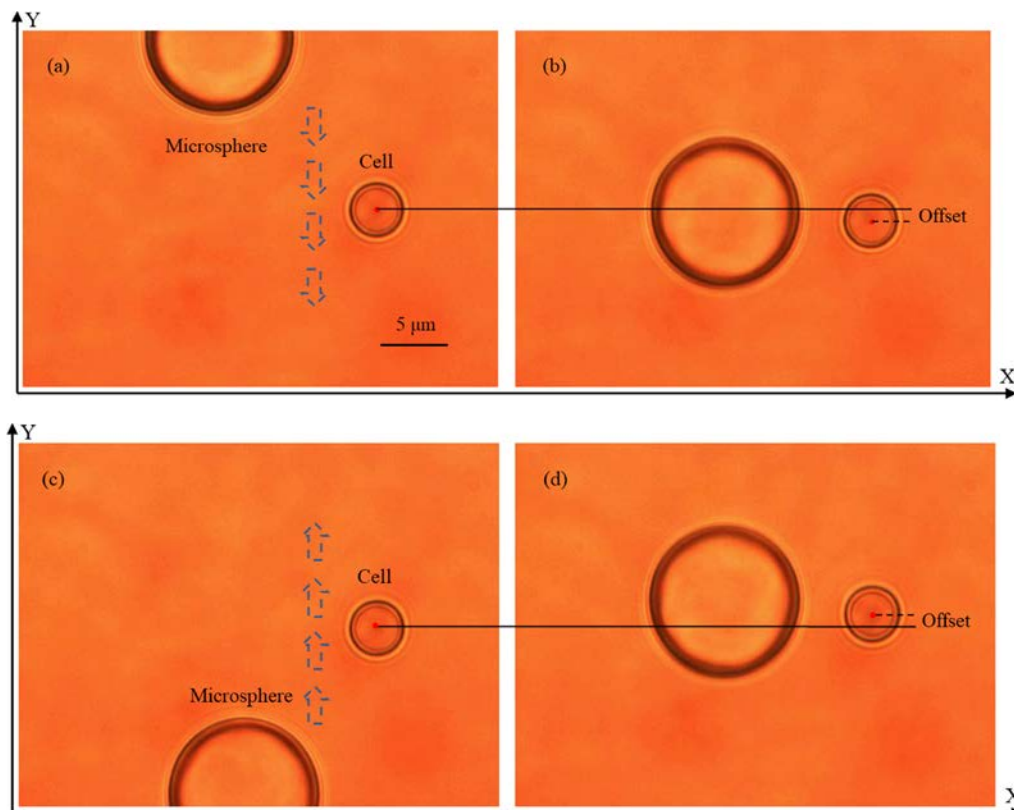


Figure 6. Quantitative measurement of microfluidic flow velocity.

Figure 7 depicts a typical example of the offsets of the cell from the optical trap under the generated microfluidic flow. In each cycle, the maximum offset was reached when the y-axis coordinates of the microsphere and the cell were identical. In Figure 7, the maximum offsets in each cycle were closed, indicating that our method used to move the microsphere achieved a high precision. When processing data, we used the absolute value of the five largest values in each cycle and then obtained the average as the result of each experiment. Ten experiments were repeated, and the mean of the absolute offset was $2.7 \mu\text{m}$. According to equations (6) and (7), we determined the microfluidic flow velocity of $27.3 \mu\text{m/s}$, which was between 25.1 and $33.5 \mu\text{m/s}$ and the same as that of the theoretical value.

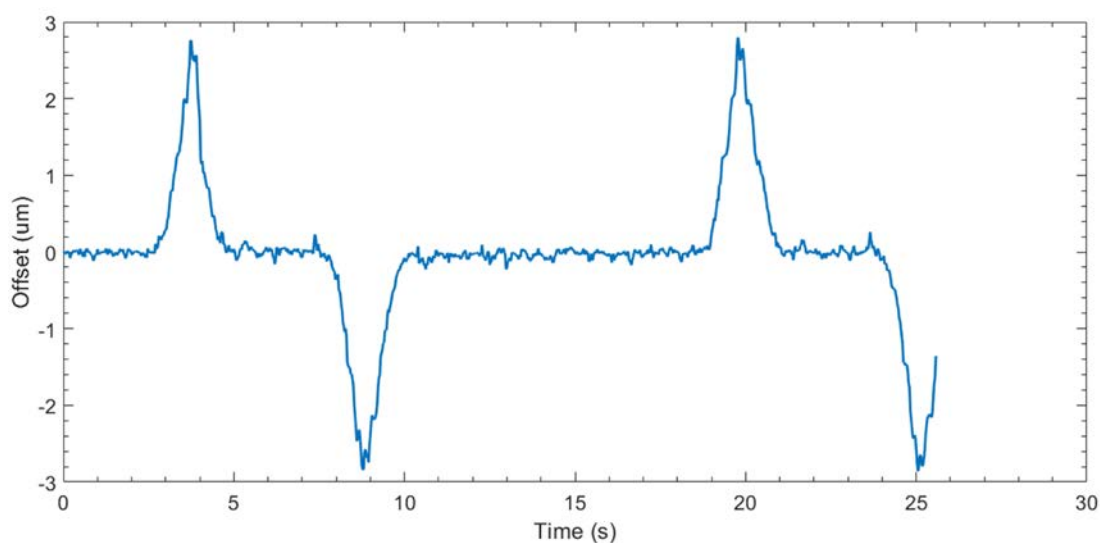


Figure 7. Offsets of the cell under the generated microfluidic flow.

4. Summary and conclusions

This study can be summarized as follows: (1) a novel approach is proposed to generate microfluidic flow quantitatively by automatically moving a microsphere in liquid via a manipulation system of HOTs. (2) A closed-loop control strategy is introduced to achieve high movement precision and robustness. (3) The theoretical solution of the generated microfluid is obtained on the basis of Stokes equations. (4) An experimental method is proposed to characterize the microfluidic flow. Experiments are performed and the experimental results are consistent with the theoretical findings, verifying the effectiveness of our approach.

This method does not impose any dedicated fabrication of microtool, and the microfluidic flow is dexterously adjustable by controlling the direction, speed, and distance of microspheres from a target location. However, our approach is limited by the relatively smaller generated fluid than those obtained using conventional methods with a syringe pump. In addition, our approach is unsuitable for applications wherein target locations are susceptible to light interference. The proposed approach shows potential for applications involving microfluidic flow actuation, investigations on cell behavior under microfluidic stimulation, and material transport in microfluidic systems.

Acknowledgments

The authors acknowledge the support from the National Natural Science Foundation of China (No. 61803270 and 61701442), and Natural Science Foundation of Guangdong Province (No. 2015A030310268).

Conflict of interest

All authors declare no conflicts of interest in this paper.

References

1. L. H. Hung and A. P. Lee, Microfluidic devices for the synthesis of nanoparticles and biomaterials, *J. Med. Biol. Eng.*, **27**(2007), 1–6.
2. P. Yager, T. Edwards, E. Fu, et al., Microfluidic diagnostic technologies for global public health, *Nature*, **442**(2006), 412–418.
3. J. Mairhofer, K. Roppert and P. Ertl, Microfluid systems for pathogen sensing: A review, *Sensors*, **9**(2009), 4804–4823.
4. M. Shamsi, M. Saghafian, M. Dejam, et al., Mathematical modeling of the function of Warburg effect in tumor microenvironment, *Sci Rep*, **8**(2018), 8903.
5. M. Shamsi, A. Sedaghatkish, M. Dejam, et al., Magnetically assisted intraperitoneal drug delivery for cancer chemotherapy, *Drug Deliv.*, **25**(2018), 846–861.
6. J. L. Li, D. Day and M. Gu, Design of a compact microfluidic device for controllable cell distribution, *Lab Chip*, **10**(2010), 3054–3057.
7. Q. Wang, L. Huang, K. Wen, et al., The mean and noise of stochastic gene transcription with cell division, *Math. Biosci. Eng.*, **15**(2018), 1255–1270.
8. R. Dhumpa and M. G. Roper, Temporal gradients in microfluidic systems to probe cellular dynamics: a review, *Anal Chim Acta.*, **19**(2012), 9–18.
9. Ahmed and J. I. Siddique, The effect of magnetic field on flow induced-deformation in absorbing porous tissues, *Math. Biosci. Eng.*, **16**(2019), 603–618.
10. M. Dejam, H. Hassanzadeh and Z. Chen, Shear dispersion in combined pressure-driven and electro-osmotic flows in a channel with porous walls, *Chem. Eng. Sci.*, **137**(2015), 205–215.
11. V. Faustino, S. O. Catarino, R. Lima, et al., Biomedical microfluidic devices by using low-cost fabrication techniques: a review, *J. Biomech.*, **49**(2016), 2280–2292.
12. K. S. Tee, M. S. Saripan, H. Y. Yap, et al., *Development of a mechatronic syringe pump to control fluid in a microfluidic device based on polyimide film*, IOP Conference Series: Materials Science and Engineering, **226**(2017), 012031.
Available from: <https://iopscience.iop.org/article/10.1088/1757-899X/226/1/012031/meta>
13. T. Bayraktar and S. B. Pidugu, Characterization of liquid flows in microfluidic systems, *Int. J. Heat Mass Transf.*, **49**(2006), 815–824.
14. M. P. Hughes, Strategies for dielectrophoretic separation in laboratory on-a-chip systems, *Electrophoresis*, **23**(2002), 2569–2582.
15. F. Petersson, L. Aberg, A. M. Swärd-Nilsson, et al., Free flow acoustophoresis: microfluidic-based mode of particle and cell separation, *Anal. Chem.*, **79**(2007), 5117–5123.

16. S. Kim and K. Ishiyama, Magnetic robot and manipulation for active locomotion with targeted drug release, *IEEE-ASME Trans. Mechatron.*, **19**(2014), 1651–1659.
17. C. Pawashe, S. Floyd and M. Sitti, Modeling and experimental characterization of an untethered magnetic micro-robot, *Int. J. Robot. Res.*, **28**(2009), 1077–1094.
18. J. Köhler, R. Ghadiri, S. I. Ksouri, et al., Generation of microfluidic flow using an optically assembled and magnetically driven microrotor, *J. Phys. D. Appl. Phys.*, **47**(2014), 505501.
19. X. Wang, X. Gou, S. Chen, et al., Cell manipulation tool with combined microwell array and optical tweezers for cell isolation and deposition, *J. Micromech. Microeng.*, **23**(2013), 075006.
20. A. Ashkin, J. M. Dziedzic, J. E. Bjorkholm, et al., Observation of a single-beam gradient force optical trap for dielectric particles, *Opt. Lett.*, **11**(1986), 288–290.
21. K. Svoboda and S. M. Block, Biological applications of optical forces, *Annu. Rev. Biophys. Biomol. Struct.*, **23**(1994), 247–285.
22. D. McGloin, Optical tweezer: 20 years on, *Phil. Trans. R. Soc. A*, **364**(2006), 3521–3537.
23. T. Yang, Y. Chen and P. Minzioni, A review on optical actuators for microfluidic systems, *J. Micromech. Microeng.*, **27**(2017), 123001.
24. A. Terray, J. Oakey and D. W. M. Marr, Microfluidic control using colloidal devices, *Science*, **296**(2002), 1841–1844.
25. S. L. Neale, M. P. MacDonald, K. Dholakia, et al., All-optical control of microfluidic components using form birefringence, *Nat. Mater.*, **4**(2005), 530–533.
26. S. Maruo and H. Inoue, Optically driven micropump produced by three-dimensional two-photon microfabrication, *Appl. Phys. Lett.*, **89**(2006), 144101.
27. U. G. Būtaitė, G. M. Gibson, Y. L. Ho, et al., Indirect optical trapping using light driven micro-rotors for reconfigurable hydrodynamic manipulation, *Nat. Commun.*, **10**(2019), 1215.
28. J. Leach, H. Mushfique, R. d. Leonardo, et al., An optically driven pump for microfluidics, *Lab Chip*, **6**(2006), 735–739.
29. T. Wu, T. A. Nieminen, S. Mohanty, et al., A photon-driven micromotor can direct nerve fibre growth, *Nat. Photonics*, **6**(2012), 62–67.
30. C. Liu, S. Li, B. Ji and B. Huo, Flow-induced migration of osteoclasts and regulations of calcium signaling pathways, *Cell. Mol. Bioeng.*, **8**(2015), 213–223.
31. B. Roy, T. Das, D. Mishra, et al., Oscillatory shear stress induced calcium flickers in osteoblast cells, *Integr. Biol.*, **6**(2014), 289–299.
32. Y. Xin, X. Chen, X. Tang, et al., Mechanics and actomyosin-dependent survival and chemoresistance of suspended tumor cells in shear flow, *Biophys. J.*, **116**(2019), 1803–1814.
33. S. Hu and D. Sun, Automatic transportation of biological cells with a robot-tweezer manipulation system, *Int. J. Robot. Res.*, **30**(2011), 1681–1694.
34. S. Hu, S. Chen, S. Chen, et al., Automated transportation of multiple cell types using a robot-aided cell manipulation system with holographic optical tweezers, *IEEE-ASME Trans. Mechatron.*, **22**(2017), 804–814.
35. S. Chowdhury, P. Švec, C. Wang, et al., Automated cell transport in optical tweezers-assisted microfluidic chambers, *IEEE Trans. Autom. Sci. Eng.*, **10**(2013), 980–989.
36. X. Li and C. C. Cheah, A simple trapping and manipulation method of biological cell using robot-assisted optical tweezers: singular perturbation approach, *IEEE Trans. Ind. Electron.*, **64**(2017), 1656–1663.

37. S. Liu, D. Sun and C. Zhu, A dynamic priority based path planning for cooperation of multiple mobile robots in formation forming, *Robot. Comput-Integr. Manuf.*, **30**(2014), 589–596.
38. X. Li, H. Yang, J. Wang, et al., Design of a robust unified controller for cell manipulation with a robot-aided optical tweezers system, *Automatica*, **55**(2015), 279–286.
39. P. Kundu, I. Cohan and D. Dowling, *Fluid mechanics*, 5th edition, Academic Press, Berlin (2012).



AIMS Press

©2019 the Author(s), licensee AIMS Press. This is an open access article distributed under the terms of the Creative Commons Attribution License (<http://creativecommons.org/licenses/by/4.0>)